A CRITICAL COMPARISON OF COMPUTED AND EXPERIMENTAL PRESSURE DISTRIBUTIONS AND FORCE COEFFICIENTS ON A BLUNTED-CONE AT ANGLE OF ATTACK

by

Eugene C. Knox

Thesis submitted to the Graduate Faculty of the

Virginia Polytechnic Institute

in candidacy for the degree of

MASTER OF SCIENCE

in

Aerospace Engineering

December, 1964

Blacksburg, Virginia

ACKNOWLEDGEMENT

The author wishes to express his appreciation to the Arnold Engineering Development Center (AEDC), Air Force Systems Command (AFSC), USAF, and to the many persons of ARO, Inc., Operating Contractor of AEDC, and in particular to those of the von Karman Facility, Hypervelocity Branch, whose assistance was instrumental in the completion of the experimental work and the preparation of this thesis. The author is especially indebted to Mr. J. Lukasiewicz, Chief of the von Karman Facility, and Mr. R. Jackson, Assistant Chief of the von Karman Facility and Manager of the Hypervelocity Branch, for their permission to use the results of the author's work as material for the thesis; to Mr. J. F. Roberts for furnishing a large part of the experimental data without which this comparison would not be possible; to Mr. Clark H. Lewis for his valuable suggestions and assistance; and to Messrs. Jack D. Whitfield and B. J. Griffith, for their encouragement in this endeavor. Finally, the author wishes to express appreciation to Messrs. Billy Z. Jenkins and Lloyd Johnson, Army Missile Command, Huntsville, Alabama, for their able work in the development of the program and for providing the GASL solutions; and to Mr. Marvin Reed, ARO, Inc., for his able assistance in programming the work to be done on the IBM 7074 Computer.

TABLE OF CONTENTS

LIST OF FIGURES

NOMENCLATURE

A	Surface area, or reference area
C_A	Axial force coefficient, $F_A/q_\infty A_{ref}$
C_D	Drag force coefficient, $D/q_\infty A_{ref}$
C_{D_n}	Nose drag coefficient (0.964 for spherical cap computed by modified Newtonian theory)
C_F	General force coefficient representing the total force acting on a vehicle
C_L	Lift force coefficient, $L/q_\infty A_{ref}$
$\overrightarrow{C_{M_o}}$	Resultant moment coefficient vector, sum of moments of all body forces about a point "0", defined by Eqn. (10), Moment/$q_\infty A_{ref} D_b$
C_m	Pitching moment coefficient
C_N	Normal force coefficient, $F_N/q_\infty A_{ref}$
C_p	Pressure coefficient, $(p_\ell - p_\infty)/q_\infty$
D	Drag force, sum of all forces acting in the windward direction, $C_D q_\infty A_{ref}$
d	Vehicle nose diameter
D_b	Vehicle base diameter
F_A	Axial force, sum of all forces acting in the body axial direction (along Z_B), $C_A q_\infty A_{ref}$
F_N	Normal force, sum of all forces acting normal to the body axial direction, $C_N q_\infty A_{ref}$
L	Lift force
M	Mach number
$\vec{n}$	Unit vector (inward) normal to a surface
p	Pressure
q	Dynamic pressure, $\rho V^2/2$
R_B	Body radius in the body axis system

R_b	Vehicle base radius
Re_∞/inch	Unit Reynolds number based on free-stream properties, $\rho V/\mu$
R_n	Vehicle nose radius
$\vec{r}$	Radius vector from point "O" to a body point
V	Velocity
X	Coordinate axis normal to Z in the vertical plane
Y	Coordinate axis normal to the XZ plane
Z	Coordinate axis in windward or body axis of symmetry direction
α	Angle of attack
γ	Ratio of gas specific heats (1.40 used herein)
ε	$(\gamma-1)/(\gamma+1)$
θ	Polar angle measured in the plane perpendicular to the axis of symmetry
ρ	Density
σ_c	Cone half-angle
μ	Gas viscosity
ψ	Bluntness ratio of nose to base radius

Subscripts

B	Body axes
b	Base
ℓ	Local
n	Nose, or normal direction
ref	reference, denotes reference area which in all cases is base area (πR_b^2)
w	Wind axes

1, 2, 3, 4 Denotes values of parameters at limits of integration for each region, at special values of Z and θ, or values of force coefficients for each like numbered region

∞ Denotes free-stream, or undisturbed flow conditions

CHAPTER I

INTRODUCTION

1. GENERAL REVIEW

The fundamental problem of general three dimensional supersonic flow-field analysis has been studied for many years, but until recently it has remained unsolved. The primary reason for this difficulty has not been due to any lack of basic theory. Rather, the complexity encountered in integrating the governing equations, as well as the quantity of numerical calculations required, were of such magnitude that hand computation was impractical, and even some of the early computing machines were inadequate. But with the rapid advance of computer technology and the increase in computer size in recent years, it has now become feasible to develop machine techniques for the numerical computation.

The need for such a capability springs essentially from two main areas of interest. First, there is interest in the programming and computing techniques which become necessary for so complex a task as computing the pressure distributions and resultant forces and moments on a vehicle in an inviscid flow field. Although several two-dimensional and axisymmetrical analyses have been developed, they are quite limited and do not apply to the non-symmetrical body, nor to axisymmetrical bodies at angle of attack. A second area of interest is that of hypersonic flight at high altitude. Vehicles operating in this flight regime are subject to strong viscous effects, with the result that the actual pressure distributions, forces, and moments

are altered by varying degrees. Considerable effort has been spent on both experimental and theoretical studies to assess the magnitudes of the viscous effects on hypersonic configurations, such as blunt slender cones. Some progress has been made in both these areas of investigation but much more research is needed, particularly in the theoretical area.

To date, the theoretical analysis of the viscous interaction phenomenon has been limited to the case of zero yaw. The presently available axisymmetrical inviscid solutions permit an analysis of the viscous boundary layer surrounding a body by using the inviscid solution as the conditions external to and influencing the development of this layer. The work of Whitfield and Griffith (1)[1] represents a significant contribution in this area. But, as they conclude, more work remains to be done in order to better understand the viscous phenomenon.

The state of the art regarding the theoretical analysis of viscous effects at angle of attack is considerably less advanced. One reason for this difficulty is that there has not been available an adequate mathematical description of the flow field about lifting bodies. This has limited the work in this area primarily to experimental studies. Therefore, the development of a general three-dimensional computer program is essential if the emphasis is to be shifted toward a more balanced analysis, from both the experimental

---

[1]Numbers in parantheses refer to references at the end of the text.

and theoretical viewpoints. A significant computer program, which should substantially improve this balance, has been developed by G. Moretti, et al., (2), at the General Applied Sciences Laboratories*, for the Aeronautical Systems Division, USAF. An evaluation of this program is the subject of this thesis.

The reader is referred to an IAS paper by Fowell (3) and an article by Ferri (4) for a more general discussion of the problems associated with general three-dimensional numerical analysis techniques as well as the limitations of "semi-three dimensional" axisymmetrical computer techniques. Moreover, reference is made here to the fact that there are two other general three-dimensional computer programs presently known to exist. One is being developed at the Lockheed Aircraft Corporation (Huntsville, Alabama), while work on the other is being done at the Northrop Aircraft Corporation (Hawthorne, California). There are no specific references to these programs in the literature and, to the author's knowledge, these programs are still in the preliminary check-out stage. The program developed by GASL has been written for the IBM 7090 computer, and has been used to obtain results for approximately six months prior to the writing of this thesis. It is, to the author's knowledge, the only workable three-dimensional program available in this country at the present time.

---

*The General Applied Sciences Laboratories (GASL) are located at Westbury, Long Island, New York. Their computer program will hereafter be referred to in this thesis as the GASL program.

2. STATEMENT OF THE THESIS

To the author's knowledge, the validity of the GASL three-dimensional computer program has not been checked by comparing its results with available experimental data, or with other programs. Of course, such checks with other programs would have to be made for certain special cases, i.e., non-lifting axisymmetrical configurations, since these are the only others presently available. Thus, in view of the program's uniqueness, it will be the subject of this thesis to compare the results from this computer program with experimental (pressure distribution and force) data on a 9-degree semivertex angle, spherically blunted cone at angles of attack ranging from zero through 20 degrees. The comparisons are made for a hypersonic Mach number of 18 and a perfect gas (γ = 1.40), although the program is sufficiently general to accept both variable Mach number as well as other values of γ. The nominal Mach number of 18 is chosen because a greater part of the experimental data are for this Mach number. However, some of the experimental data included are for a Mach number of 13, but as the data comparisons will indicate, the pressure coefficient becomes essentially independent of Mach number above a value of 10.

Although the GASL program considers only a non-viscous gas, the experimental data available for comparison do have viscous effects, hence the best agreement is not obtained in these comparisons. Therefore, some discussion relating to the viscous effects is presented to explain the differences.

3. PROCEDURE

The computational procedure of the present analysis consists of operating on the output of the GASL program to transform it to a more standard form in order to provide a comparison with experimental data. The GASL program computes flow quantities at several points in the flow field, between the body and the shock, along rays which lie in a plane perpendicular to the free-stream velocity. Hence, at angles of attack (other than zero), the radial surface pressure distribution is known in a plane which is inclined to the body axis. The experimental pressure distributions, however, were recorded in planes normal to the body axis at all angles of attack. The GASL computed results have been transformed to the body axis system by a 4-point LaGrangian interpolation formula which yields a pressure distribution that is directly comparable with the experimental data. Furthermore, the theoretical pressure distribution has been integrated by the trapezoidal rule to obtain the pressure forces acting on the body, and these are also compared with experimental data. All computations to be performed on the GASL program output were programmed for the IBM 7074 computer.

Also, in view of their wide use, and for purposes of comparison, computations of pressure distributions were made using the modified Newtonian theory. These results are presented as pressure distributions and force coefficients which are compared with both the GASL theoretical results and the experimental data. The comparison of the pressure distributions and force data are presented for angles of attack of 0, 5, 10, 15, and 20 degrees, respectively.

CHAPTER II

INVESTIGATION

1. THEORETICAL PROGRAM

GASL Computer Program

The computer program developed by the General Applied Science Laboratories and used in this analysis is a full 32,000 word program with overlaying requirements to meet the size limitations of the IBM 7090 computer. In deference to the program's size and complexity, no attempt has been made here to dissect and analyze the computer techniques used. Too, it has not been felt necessary to become familiar with all the analytical details of the program; rather, the author is concerned with its application to a specific problem area. A unique feature of this program is that it works; hence the question considered in this thesis is, "How well does it work?" Therefore, this section is only a brief description of the analytical and computer techniques used in the program, which distinguish it from others that may now exist or be developed in the near future.

The GASL computer program utilizes the method of characteristics to compute the fluid properties in the inviscid, supersonic, three-dimensional flow field about spherically-capped, arbitrarily shaped lifting bodies. The computations may be made for a perfect gas or for real air in thermodynamic equilibrium. The limitations to be considered are that no large local expansions, such as sharp corners, can exist; no secondary shock systems can be present; and no cases where separated regions may be present in the flow field can be

considered.

The computational technique is such that the calculations are made for "wind axes"; i.e., in planes perpendicular to the direction of the free-stream velocity vector. In the present case an axisymmetrical body at angle of attack is considered, so that a cylindrical coordinate system is used, i.e., for a given Z_W plane, points in the flow field, between the shock and the body surface, are described by a meridinal angle and a radius length. The number of points may be refined to 20 points between the body and shock and 30 increments in angle between the windward and leeward sides of the body. The number of Z_W planes at which solutions are obtained is dependent on the characteristics net and the number of points known in the initial plane. For the present case, 11 points along rays of 10-degree increments have been used in the analysis.

In this particular application, the computational procedure detailed in (2) has been modified in that the input data for the supersonic solution is derived from a program written by the Space General Corporation (5) for the Aeronautical Systems Division, USAF, which uses the van Dyke inverse method (6), rather than the method discussed in (2). Moreover, an attempt has been made to circumvent the restriction of no separated regions by terminating the computing procedure before the separation region is reached, and a comparison is made of these results with experimental data for the same conditions where separation is assumed to have occurred. Hence, only by a critical examination of these comparisons can some measure of the program's

validity and limitations be made.

The origin of the coordinate system is chosen to be at the center of the spherical cap as shown in Figure 1. Also shown is the dashed line along which the calculations are made. At each "jump" in X_w a change of frame of reference is made in order to keep the axis system near the axis of symmetry of the body. This is necessary to prevent the solution from becoming double valued as well as distorted

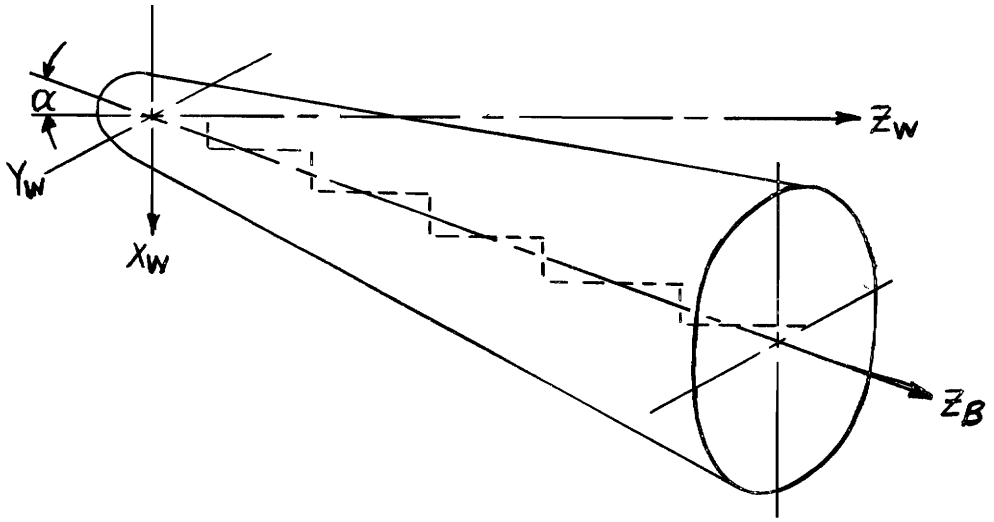

Note: Z_B coplanar with Z_w

Figure 1. Sketch of the Coordinate System Used in the GASL Program

whenever Z_w pierces the body surface. The user has the capability of scheduling the frame changes in any desired manner so long as it is consistent with the chosen coordinate system. The coordinate system will be specified, depending on the body geometry, in which case there

is a subroutine available which may be modified for radically different type bodies, such as a slab delta wing. Only the concepts of a "plane slice" perpendicular to Z_w and the spherical cap must be retained in the program.

Some of the required inputs to the program are the free-stream conditions, specified values of Z_w at which frame changes occur, the initial-plane fluid properties, and operational data such as the number of points desired between the body and shock, the angle increments chosen, etc. The data output consists of the three velocity components, their derivatives, the point radius-vector magnitude, speed of sound, entropy, density, pressure, enthalpy, and x, y coordinates for each point between the body and the shock. These values are non-dimensionalized with respect to various constants characteristic of the particular flow field and geometry, i.e., stagnation conditions, nose radius, etc. Through a control number, N, one can have recorded on the output tape every Nth plane, which is in turn printed out on paper. Likewise, a similar control number manipulates the output to be recorded on another output tape for every specified number of steps in Z_w and at every frame change. In this regard, at a later time the program may be restarted at one of these planes, using this output tape for the subsequent run. This control feature can save computer time should the program fail at some point in the calculations. In some cases only a modification of the desired points is necessary from that station on downstream in order to enable the program to proceed from the failure point. This feature will be discussed more fully in a

subsequent chapter.

Analysis Program

The primary interest in this analysis has been in the surface pressures as computed by the GASL program, and the resultant forces derived from these pressures. The GASL output pressure data are given in atmospheres, and because the computations are programmed in the wind-axis system, the pressure distributions are computed in planes other than those perpendicular to the body's axis of symmetry - the form in which the experimental pressure distributions are recorded. In order that a direct comparison can be made, it is necessary to transform the computed pressures to the body planes. Moreover, due to the perponderous amount of computed data and the desire for better accuracy, it was decided that a computer program should be written to transform the pressures and print out distributions at desired body planes. These would then be integrated to obtain the inviscid force and moment coefficients. The discussion which follows is a description of the derivation of the equations used in the computer program.

It can be seen from Figure 1, page 15, that the two axes systems of interest are related by a transformation, which is presented in the following matrix form:

$$[X_W, Y_W, Z_W] = \begin{bmatrix} \cos\alpha & 0 & \sin\alpha \\ 0 & 1 & 0 \\ -\sin\alpha & 0 & \cos\alpha \end{bmatrix} [X_B, Y_B, Z_B] \qquad (1)$$

In the body-axis system, the X and Y coordinates are replaced by the polar coordinates R_B and θ_B, so that

$$X_B = \left(\frac{R_B}{R_n}\right)\cos\ \theta_B, \qquad Y_B = \left(\frac{R_B}{R_n}\right)\ \sin\ \theta_B, \tag{2}$$

where X_B and Y_B are nondimensionalized with respect to the nose radius. Using equation (2) in the scalar form of equation (1) one finds that

$$\left.\begin{aligned} X_w &= \left(\frac{R_B}{R_n}\right)\ \cos\ \theta_B\ \cos\alpha + Z_B\ \sin\ \alpha \\ Y_w &= Y_B \end{aligned}\right\} \tag{3}$$

and

$$Z_w = Z_B\ \cos\ \alpha - \left(\frac{R_B}{R_n}\right)\ \cos\ \theta_B\ \sin\ \alpha.$$

The geometry is such that

$$\theta_B \equiv \tan^{-1}\left(\frac{Y_B}{X_B}\right), \quad \theta_w \equiv \tan^{-1}\left(\frac{Y_w}{X_w}\right)$$

or, in the case of θ_w,

$$\theta_w = \tan^{-1}\left[\frac{\left(\frac{R_B}{R_n}\right)\ \sin\ \theta_B}{\left(\frac{R_B}{R_n}\right)\ \cos\ \theta_B\ \cos\ \alpha + Z_B\ \sin\ \alpha}\right],$$

so that

$$\left.\begin{aligned} Z_w &= Z_B\ \cos\ \alpha - \left(\frac{R_B}{R_n}\right)\ \cos\ \theta_B\ \sin\ \alpha \\ \text{and} \\ \theta_w &= \tan^{-1}\left[\frac{\left(\frac{R_B}{R_n}\right)\ \sin\ \theta_B}{\left(\frac{R_B}{R_n}\right)\ \cos\ \theta_B\ \cos\ \alpha + Z_B\ \sin\ \alpha}\right] \end{aligned}\right\} \tag{4}$$

represent the transform equations from body axes to wind axes.

Inasmuch as the reference axis for θ_w, within each frame change, is the shifted Z_w axis, there is a correction on X_w in computing tan θ_w. This correction is obtained by decreasing X_w by the amount of the sum of the ΔX_w's for all frame changes up to the point considered, so that equations (4) became

$$\left.\begin{aligned} Z_w &= Z_B \cos\alpha - \left(\frac{R_B}{R_n}\right)\cos\theta_B \sin\alpha \\ \text{and} \quad \theta_w &= \tan^{-1}\left[\frac{\left(\frac{R_B}{R_n}\right)\sin\theta_B}{\left(\frac{R_B}{R_n}\right)\cos\theta_B\cos\alpha + Z_B\sin\alpha - \sum_{i=1}^{m}\Delta X_{wi}}\right] \end{aligned}\right\}, \qquad (5)$$

where m represents the number of frame changes which have occurred up to that point. Equations (5) are those used to determine the equivalent Z_w and θ_w for a given Z_B and θ_B and the associated pressures on the body surface. The technique used to describe the pressure at a given point is a LaGrangian 4-point interpolation formula of the form

$$Y = F_1(x)Y_1 + F_2(x)Y_2 + F_3(x)Y_3 + F_4(x)Y_4,$$

where

$$F_1(x) = \frac{(x-x_2)(x-x_3)(x-x_4)}{(x_1-x_2)(x_1-x_3)(x_1-x_4)}, \quad F_2(x) = \frac{(x-x_1)(x-x_3)(x-x_4)}{(x_2-x_1)(x_2-x_3)(x_2-x_4)}$$

$$F_3(x) = \frac{(x-x_1)(x-x_2)(x-x_4)}{(x_3-x_1)(x_3-x_2)(x_3-x_4)}, \quad F_4(x) = \frac{(x-x_1)(x-x_2)(x-x_3)}{(x_4-x_1)(x_4-x_2)(x_4-x_3)}$$

The subscript numbers represent the known values to be interpolated in both Z_w and θ_w. More specifically, for a chosen Z_B and θ_B, the

corresponding Z_w and θ_w were first computed. The computer then searched the GASL results for four sets of pressures which bracketed both Z_w and θ_w, preferably 2 on each side (as the end of the body or a frame-change was approached, a 3 and 1 or an end point interpolation was performed). In all, five interpolations were necessary to define the pressure at a point; that is, four were required to determine the pressure at each of the four known θ_w's in the desired Z_w plane, and a final interpolation on θ_w yielded the desired result. In the present analysis, these calculations are performed at 0.2 intervals in Z_B, beginning at -1 and ending at 14.644, with additional special Z_B values investigated for comparison purposes. In each Z_B plane pressures are computed at each 10° increment in θ_B. The resultant pressures are printed out and stored for integration in the force equations (a derivation of these expressions is presented below).

A general expression for the resultant force coefficient acting on a body due solely to the surface pressure may be written as:

$$\overrightarrow{C_{F_n}} = \iint_A \frac{C_p \, \vec{n} \, dA}{\pi R_b^2} , \qquad (6)$$

where πR_b^2 is the base reference area, C_p the local pressure coefficient, and $\vec{n}$ the local (inward) unit normal vector for an element of surface area dA. As can be readily seen, the normal vector and the elemental area are functions of the local body geometry. Thus, for the present case, equation (6) might well be evaluated for only two regions, the spherical cap and the conical afterbody. However, for ease of computing, three regions are chosen, as shown in Figure 2, page 21. In

regions 1 and 2, the integration was performed in the wind axis system because these regions are for a sphere at zero angle of attack.

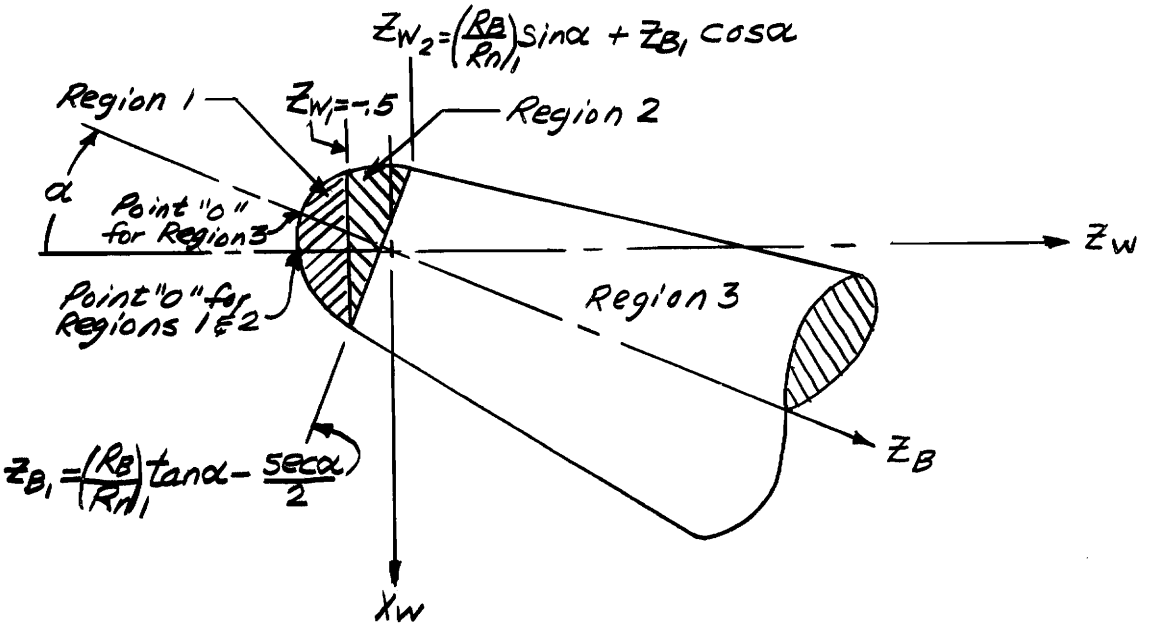

Figure 2. Sketch of Model Showing Three Regions of Integration

In these regions C_p is constant for a given Z_w. It follows immediately that, in region 1,

$$(C_{F_{Z_w}})_1 = -2\left(\frac{R_n}{R_b}\right)^2 \int_{-1}^{Z_{w1}} C_p\, Z_w\, dZ_w \qquad (7)$$

The net force acting in the X_w or Y_w direction is zero in region 1.

The resulting equations for region 2 are different from

those in region 1 only because the lower limit of integration is determined by the plane Z_{B_1}. For any selected value of Z_w, the intersection of this Z_w plane with the Z_{B_1} plane determines the lower limit on θ_w, as well as a value of θ_{B_1} in the region 2 calculations. With both Z_w and Z_{B_1} known, then,

$$\theta_{B_1} = \cos^{-1}\left[\frac{Z_w - Z_{B_1}\cos\alpha}{-\left(\frac{R_B}{R_n}\right)_1 \sin\alpha}\right]$$

where

$$\left(\frac{R_B}{R_n}\right)_1 = \sqrt{1 - Z_{B_1}^2}$$

and

$$\theta_{w_1} = \tan^{-1}\left[\frac{\left(\frac{R_B}{R_n}\right)_1 \sin\theta_{B_1}}{\left(\frac{R_B}{R_n}\right)_1 \cos\theta_{B_1}\cos\alpha + Z_{B_1}\sin\alpha}\right]$$

Hence, the range of integration in θ_w is from θ_{w_1} to $-\theta_{w_1}$. Also, in region 2 there is a net normal force along the X_w axis. The equations for these force coefficients in region 2 are as follows:

$$\left.\begin{aligned}(C_{F_{Z_w}})_2 &= -\frac{2}{\pi}\left(\frac{R_n}{R_b}\right)^2 \int_{Z_{w_1}}^{Z_{w_2}} C_p\, Z_w\, \theta_{w_1}\, dZ_w \\ \text{and} \\ (C_{F_{X_w}})_2 &= \frac{2}{\pi}\left(\frac{R_n}{R_b}\right)^2 \int_{Z_{w_1}}^{Z_{w_2}} C_p \sqrt{1 - Z_w^2}\, \sin\theta_{w_1}\, dZ_w\end{aligned}\right\} \quad (8)$$

In region 1, the values of C_p are taken from the Space-General solution (Ref. 5), and then used to compute the input conditions for the GASL program. In region 2, the values obtained from the GASL program are used. In region 3, C_p is not constant with respect to either θ_w or θ_B, so there is no advantage in continuing the integration in the wind axis system; moreover, from a geometrical point of view, the equations are more tractable in the body axis system. So, in equation (6), the expression for the inward unit normal vector at any point on the cone is substituted and the integration performed, yielding to the results

$$\left.\begin{aligned}(C_{F_{Z_B}})_3 &= \frac{2}{\pi}\left(\frac{R_n}{R_b}\right)^2 \tan\sigma_c \int_{Z_{B_1}}^{Z_{B_{max}}} \left(\frac{R_B}{R_n}\right)\left\{\int_0^{\theta_{B_{max}}} C_p \, d\,\theta_B\right\} dZ_B \\ \text{and} \\ (C_{F_{X_B}})_3 &= -\frac{2}{\pi}\left(\frac{R_n}{R_b}\right)^2 \int_{Z_{B_1}}^{Z_{B_{max}}} \left(\frac{R_B}{R_n}\right)\left\{\int_0^{\theta_{B_{max}}} C_p \cos\theta_B \, d\,\theta_B\right\} dZ_B\end{aligned}\right\} \quad (9)$$

In region 3, the GASL results are interpolated for a selected Z_B, and then the integrals in θ_B evaluated by the trapezoidal rule. Next, these values are integrated along the body length, by the trapezoidal rule, to obtain the coefficients in equation (9). Due to the large number of Z_B planes employed (150), it is felt that this integration technique is sufficiently accurate.

For all three regions it can be shown, mathematically, that the side force integrates to zero. Physically one can see that due to

symmetry the incremental side forces cancel one another, leading to the zero resultant.

The general equation for the moment coefficient about a chosen point "O" may be expressed as

$$(\vec{C_M})_o = \iint_A \frac{\vec{r} \times C_p \vec{n}\, dA}{(\pi R_b^2)\, D_b} \quad , \tag{10}$$

where $\vec{r}$ is the radius vector from the point "O". For regions 1 and 2, the point "O" is chosen as the intersection of Z_w with the sphere (see Fig. 2), so that

$$\left.\begin{aligned} (C_m)_{O,1} &\equiv 0 \\ (C_m)_{O,2} &\equiv (C_{F_{X_w}})_2 \left(\frac{R_n}{D_b}\right) \end{aligned}\right\} \tag{11}$$

The latter result in Eqs. (11) is obtained because the resultant moment arm for the forces in region 2 is unity. In region 3, the point "O" is taken as the intersection of Z_B with the sphere, so that

$$(C_m)_{O,3} = -\frac{2}{\pi}\left(\frac{R_n}{R_b}\right)^2 \left(\frac{R_n}{D_b}\right) \left\{ \int_{Z_{B_1}}^{Z_{B_{max}}} \left(\frac{R_B}{R_n}\right) \int_0^{\theta_{B_{max}}} C_p \cos\theta_B \, d\theta_B \right\} \tag{12}$$

$$\left[(Z_B + 1) + \left(\frac{R_B}{R_n}\right) \tan\sigma_c \right] dZ_B$$

To add all the contributions of the several regions, the coefficients in regions 1 and 2 are transformed to region 3 through the angle of attack, so that the final expressions for the normal and axial force, pitching moment coefficients, and for the center of pressure location

from the nose* are obtained as

$$\left.\begin{aligned} C_A &= \left[(C_{F_{Z_w}})_1 + (C_{F_{Z_w}})_2\right] \cos\alpha + (C_{F_{X_w}})_2 \sin\alpha + (C_{F_{Z_B}})_3 \\ C_N &= \left[(C_{F_{Z_w}})_1 + (C_{F_{Z_w}})_2\right] \sin\alpha + (-C_{F_{X_w}})_2 \cos\alpha - (C_{F_{X_B}})_3 \\ C_{m_{nose}} &= (C_m)_{0,3} + \left[(C_{F_{X_w}})_2 \cos\alpha - (C_{F_{Z_w}})_2 \sin\alpha\right]\left(\frac{R_n}{D_b}\right) \\ X_{cp}/D_b &= C_m/C_N \end{aligned}\right\} \quad (13)$$

Moreover, in order to compute the lift to drag ratio, the following relations are used

$$\left.\begin{aligned} C_L &= C_N \cos\alpha - C_A \sin\alpha \\ C_D &= C_A \cos\alpha + C_N \sin\alpha \end{aligned}\right\} \quad (14)$$

and

$$L/D = C_L/C_D \quad (15)$$

These final equations yield the results from the GASL program which have been used to compare the computed force and moment coefficients with experimental data. These comparisons are presented in a later chapter; however, a discussion of the experimental investigation is presented first.

---

*Pitching moment and center of pressure location are referenced to the point "O" where Z_B intersects the sphere.

2. EXPERIMENTAL PROGRAM

The experimental data presented herein were obtained in investigations conducted at two separate laboratories, the Arnold Engineering Development Center (Tullahoma, Tennessee), and the Cornell Aeronautical Laboratory (Buffalo, New York). These data are for a spherically capped, 9-degree semivertex angle cone with a nose-to-base radius ratio of 0.3. Originally, this model configuration was designed to study the presence of viscous effects at the available wind tunnel test conditions. However, the large amount of data available for this configuration has made it attractive for comparison purposes even with the inviscid computer solution. In the Mach number range considered, these data from CAL and AEDC are the only such information available in the literature (to date) for this configuration.

The AEDC experiments were conducted in the von Karman Gas Dynamics Hypersonic Tunnel H (a 50-inch diameter hotshot tunnel) and Tunnel F (a 100-inch diameter hotshot tunnel). In these facilities energy is added to a small volume of gas (known mass) by means of a high-current electric arc. The controlled energy addition raises the pressure to a desired maximum value. Typical values of maximum stagnation pressure and temperature for the data presented here are 14,000 psia and 2500°K, respectively. During pressure rise, a diaphragm located downstream of the throat ruptures at a controlled pressure. The gas is then allowed to expand into the test section through a conical nozzle. The expansion lowers the total pressure continuously

during the run. Also, the expansion is considered isentropic. The Mach number is varied by changing the throat diameter. Useful run time of 20 to 50 milliseconds can be obtained on a typical run. Associated with the electric arc heater is the introduction of some particle contamination into the test section flow; however, by limiting the stagnation enthalpy to equivalent velocities of 10^4 fps, and using nitrogen as the test gas, both the amount and the effects of particle contamination are kept to tolerable levels. A complete discussion of the development of the hotshot tunnel as a reliable testing device is given by Lukasiewicz, et. al., (7).

The relatively short run time associated with a hotshot facility has necessitated the development of special measuring devices. To measure model surface pressures a variable-reluctance wafer transducer has been developed by Smotherman (8). The aerodynamic forces are measured by an ordinary strain-gage type balance, but one which has been designed to compensate for any sting accelerations. The compensation technique is described by Edenfield and Ledford in Reference (9). Finally, due to the time variation of the flow conditions, a continuous operations record is made for each run; the equipment needed for this is described by Earheart and Bynum (10), and the method by which the stagnation and test section flow conditions at any time during the useful run are computed is presented by Grabau, et. al., (11).

The Cornell test facility is a 48-inch hypersonic shock tunnel which uses a constant-area reflected shock tube to raise air to approximately the desired stagnation conditions. This air is then

expanded through a contoured nozzle to the desired test conditions. Test times of 2 to 4 milliseconds are characteristic for the tests presented here. The stagnation conditions are determined from measurements of the pressure behind the reflected shock and the speed of the incident shock. A detailed description of the tunnel's operation is given in Reference (12).

During these particular tests, peizoelectric crystals were used for pressure and force measurements; and, the data presented for force measurements have been corrected for sting accelerations. A general discussion of shock tunnel instrumentation is presented by Martin, et. al., in Reference (13).

The range of test conditions, for the data from the two facilities, are as follows:

AEDC-VKF: $16 \leq M \leq 22$; $4000 \leq Re_\infty/inch \leq 63{,}000$; $0 \leq \alpha \leq 40$-deg.

CAL: $14 \leq M \leq 15$; $2000 \leq Re_\infty/inch \leq 20{,}000$; $0 \leq \alpha \leq 40$-deg.

The Tunnel H data presented herein from the AEDC-VKF investigation were obtained by Mr. J. F. Roberts, of the Hypervelocity Branch, von Karman Gas Dynamics Facility. These results are documented in an unpublished internal laboratory report. The Tunnel F results were obtained by the author and have been documented in a similar manner. The Cornell Laboratory data have been taken from the work by Wilkinson and Harrington (14); an experimental comparison of some of the AEDC-VKF and CAL data is presented by Edenfield (15).

CHAPTER III

RESULTS AND DISCUSSION

1. COMPARISONS AT ZERO-LIFT ANGLE

It has been pointed out by Fowell (3) that for symmetrical bodies under conditions of zero yaw the flow field is rotationally symmetric and can be solved by existing axisymmetric two-dimensional theories with a high degree of accuracy. This being the case, then, it is unnecessary to use the GASL program for such problems. However, as a check of validity it is interesting to compare the GASL three dimensional program results with two-dimensional theories at zero yaw to determine how well the GASL program "collapses" into the axisymmetric case. Figure 3, page 30, shows a comparison of the GASL results with those from a program written at AEDC and one from Space-General. The AEDC and Space-General results are shown as one because, although the programs are completely separate, the results for the present case are practically identical. The correlation parameters used in Figure 3 are those first suggested by Cheng, but modified by replacing $p/M_\infty^2 p_\infty \gamma$ with $C_p/2$, as was done by Griffith and Lewis (16) to obtain better correlation. Also shown on the same figure are experimental data from AEDC-VKF and CAL tests. The AEDC-VKF Tunnel F data have been averaged to provide only one point at each body station. There were a total of 23 runs in the Tunnel F data, with a spread of approximately $\pm$ 10 percent overall, which is well within the scatter shown here.

It is noted from Figure 3 that the GASL solution is approximately 15 percent below the AEDC and Space-General solutions, and that

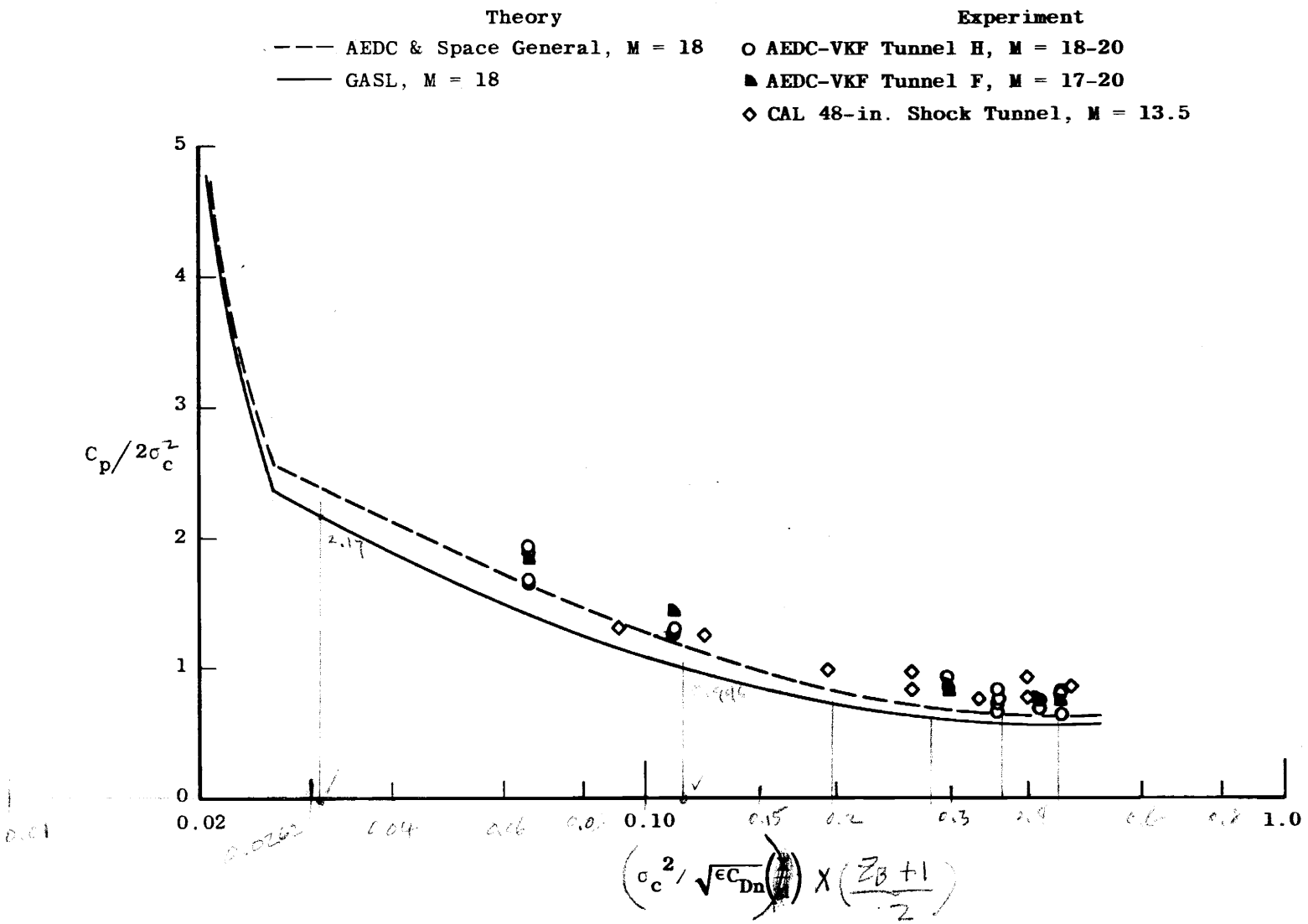

Figure 3. - Zero-lift Cone Pressure Distribution

these latter two solutions agree best with the experimental data. The deficiency of the GASL solution can be explained qualitatively by a simple comparison of the GASL and AEDC programs. As pointed out by Fowell (3), the GASL solution does not proceed along a characteristic surface; rather, characteristic lines are constructed in a radial θ_w plane from known points in the previous Z_w plane. The intersection of these characteristic lines at a downstream Z_w plane represents a possible solution. This procedure is repeated for all desired θ_w planes, and the solutions in the new Z_w plane used to obtain the solution in a subsequent Z_w plane by repeating the above procedure. The similar intersections for all subsequent radial planes would in all likelihood not occur in the same Z_w plane; therefore, an interpolation and extrapolation procedure has been adopted so as to obtain all solutions in one Z_w plane. Of necessity, such a scheme requires a relatively loose convergence criterion. However, in the case of the AEDC-VKF program, the equations are written along the characteristic lines, so that if the solution at a field point does not converge within a strict limit, the interval between the two generating points is halved and another point is sought. This technique generates more known points in the field from which the solution is inherently more accurate.

While it is felt that this provides a likely explanation for the difference between the theories, no attempt has been made to check it at this time because this would require an examination of the interior of the GASL program - a situation which is both too cumbersome and time consuming at present.

The differences between the experimental data and the AEDC-VKF or Space-General solutions have been well documented by several independent investigations for cone bodies of varying bluntness. Griffith and Lewis (16) showed the correlation presented in Figure 3 using a multitude of data for a wide range of conditions which substantiates both the correlation parameters and the differences shown here. Using the theory employed by Whitfield and Griffith (1), the analysis of Probstein (17) was used to show that viscous interaction would increase theory about 12 percent at the station closest to the nose and about 3 percent nearest the base. This still does not account for all the differences between theory and experiment; Probstein noted that his analysis was only a first order theory. It is felt that more rigorous analysis of the viscous phenomenon is required in order to substantiate these differences. Research is presently being carried out in this area by C. H. Lewis of ARO, Inc.; the preliminary results of this investigation indicate that the differences shown here are reasonable.

Hence, for present purposes it is sufficient to state that the present axisymmetrical theories are adequate, and that good agreement with experiment is obtained whenever viscous effects are properly considered. Furthermore, in view of the more lax convergence requirements in the GASL program, the differences shown between this program and the axisymmetrical theories can be accounted for, and these differences for zero-yaw conditions do not necessarily preclude applicability of the GASL program at angle of attack.

2. COMPARISONS AT ANGLE OF ATTACK

It has been shown in the previous section that for the range of flow conditions, for which experimental data are shown, blunted cone configuration has a pressure distribution which is affected by viscous phenomena. But since it is the only data available, it is necessary to examine this relatively large collection of data at angle of attack as a comparison for the GASL program. In evaluating these comparisons, qualitative consideration of the viscous effects has been made in order to identify whether or not differences should be credited to the GASL results or to the viscous interaction. It has been observed that under conditions of zero yaw a significant improvement in the agreement, between experiment and the axisymmetrical theory, has been obtained for larger-angle semivertex angle cones under similar flow field conditions. Hence, in the present case the viscous effects are expected to diminish, at least on the windward side, with increased angle of attack.

Shown in Figure 4(a), page 34, are the computed and experimental longitudinal pressure distributions on the most windward (θ_w = 0) and the most leeward ($\theta_w = \pi$) body meridians for angles of attack of 5 and 10 degrees. On the windward side, the agreement between the experimental data and the GASL results are somewhat improved over the zero yaw comparison. Moreover, inasmuch as the agreement improved markedly for the 10 degree case, it is felt that the differences shown are primarily due to viscous effects. It is gratifying to note that the trends of the theory and experiment are very similar.

On the leeward side the comparisons are not as good. It is

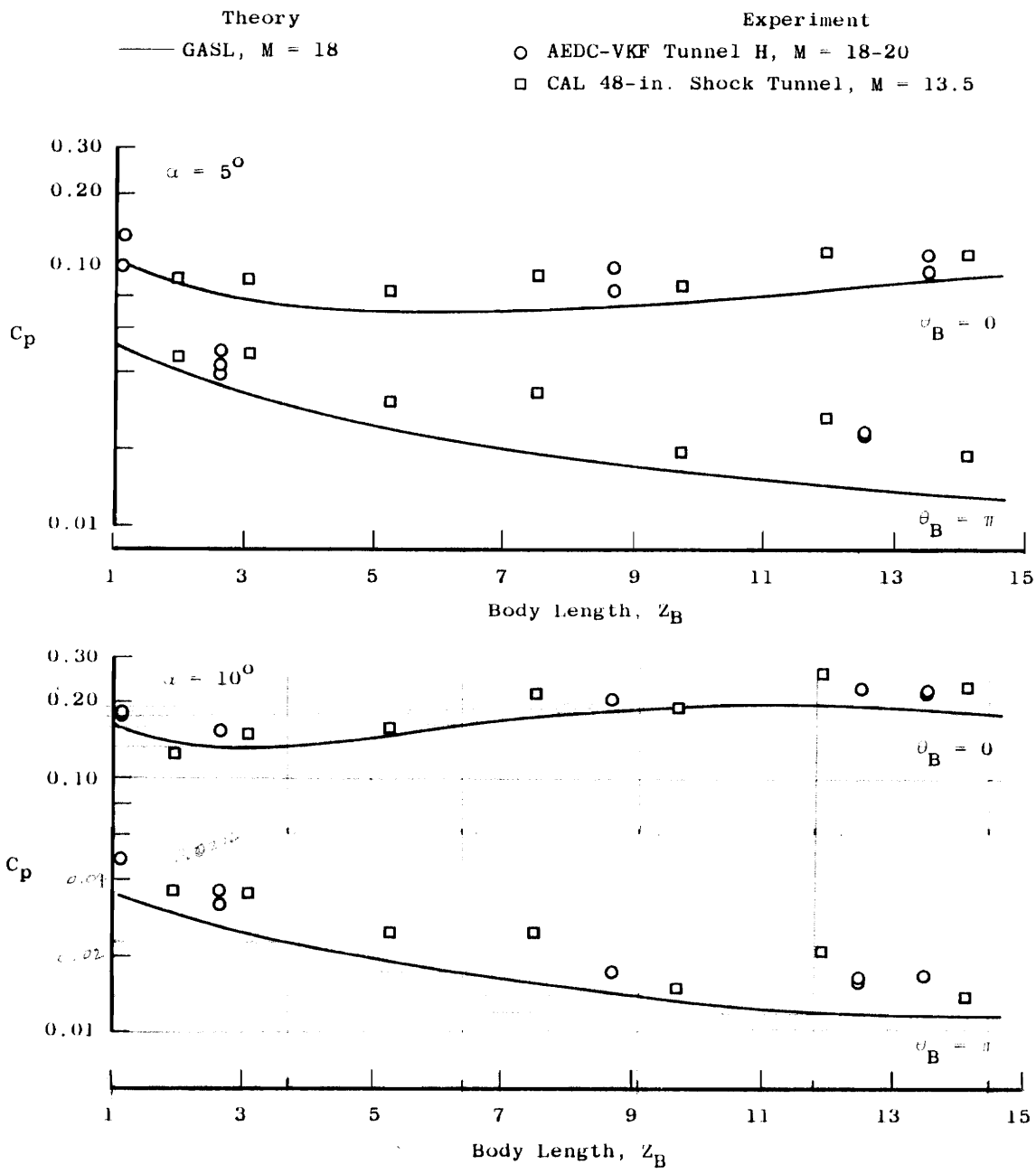

4(a) α = 5 and 10 degrees

Figure 4. - Cone Longitudinal Pressure Distributions

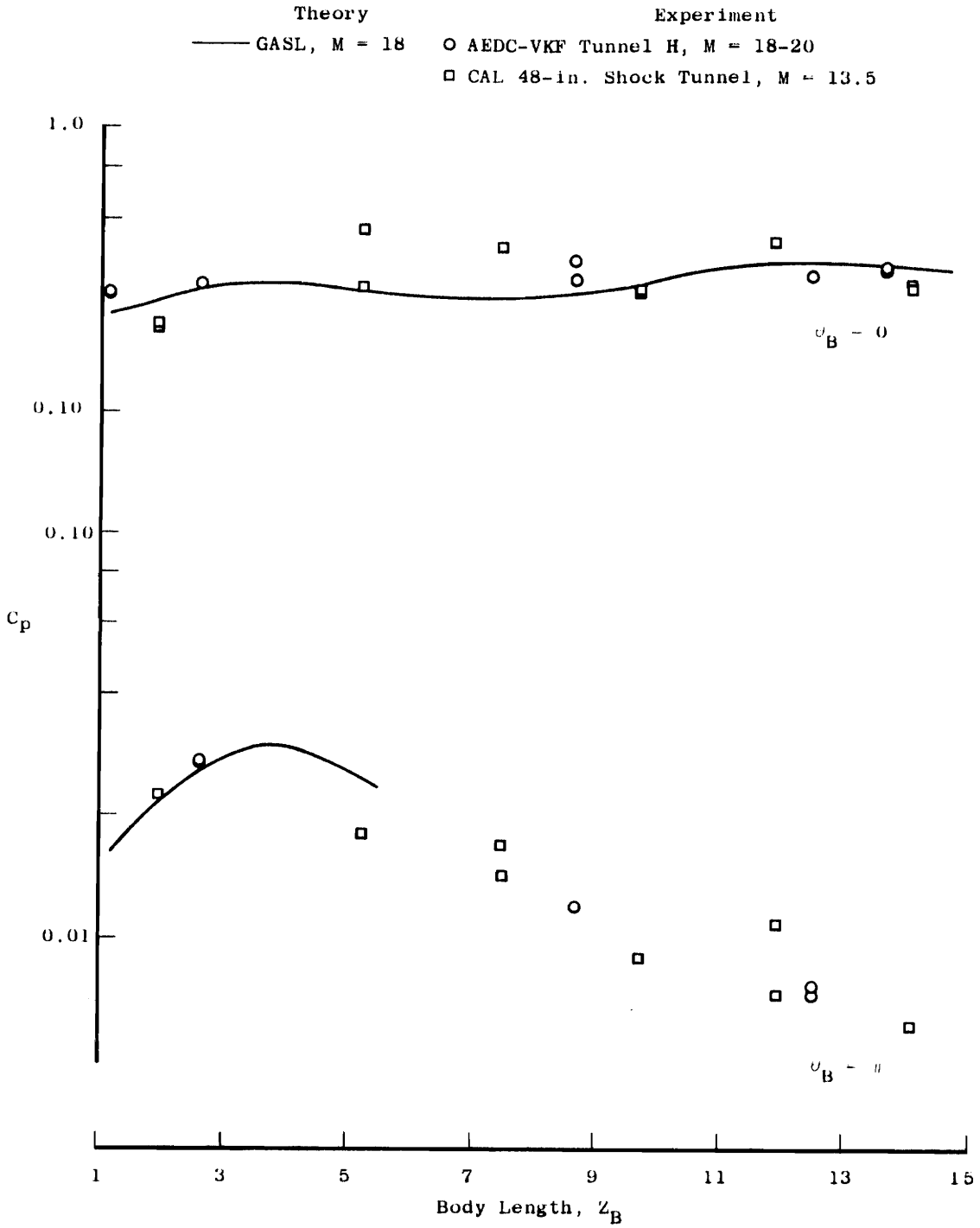

4(b) α = 20 degrees

Figure 4. - Concluded

believed that the viscous effects will tend to be amplified in this region, due to the thickening of the boundary layer, in the favorable pressure field, thereby "inducing" higher surface pressures.

A similar comparison for 20 degrees angle of attack is presented in Figure 4(b), page 35. It is noted that on the leeward side it has been necessary to "cut off" the computations, at θ_w = 130 degrees, beyond the body station shown since the solution failed to converge and indicated a negative pressure. The "cut off" was accomplished by modifying the computer input and restarting the program from the output tape just upstream of the failure point. The computations are continued on the windward side (to θ_w = 130 degrees) to the end of the body. The GASL results agree with the experimental data on the windward side reasonably well, taking into account data scatter, but not as clearly indicating the presence of viscous effects as in the previous cases.

At the time computations were made for the 20 degree angle of attack case, any failure which occurred on the leeward side of the body was construed as possible evidence of a separated region, i.e., a violation of the third program restriction (i.e., no case where flow separation exists should be considered). Hence, it was concluded that this restriction could possibly be circumvented by "cutting off" the calculations before the separated region was reached. However, subsequent comparisons with experiment have shown this not to be the case at all, as indicated by the experimental data for the leeward side in Figure 4(b), page 35. These data indicate an attached flow, so that

the failure in the GASL program was caused by something else. As subsequent comparisons will indicate, the radial pressure distributions - as the failure point was approached - were well behaved and these particular computations are not suspect. Some speculation as to the origin of this failure will be discussed in a later section of this chapter.

The radial pressure distributions, at several body stations, are shown in Figures 5, 6, 7, and 8, on pages 39 through 45, for angles of attack of 5, 10, 15, and 20 degrees, respectively. Although experimental pressure data are not available for a comparison in this instance, the 15-degree angle of attack case is presented for information purposes and to show the development of the instability encountered in the GASL solutions. This instability forced a cut-off of the computations at θ_w = 140 degrees for α = 15 degrees at Z_w = 11. The nature of the failure in this case is identical to that of the 20-degree case, except that this latter failure occurs further aft on the body.

In addition to the GASL solution, the surface pressures were obtained from the modified Newtonian theory, which can be expressed as

$$C_p = C_{p\ stag} \cos^2 \eta. \tag{16}$$

Here $C_{p\ stag}$ is the pressure coefficient at the forward stagnation point on a blunt body, which is taken to be 1.87 in this analysis, based on Mach 18 free-stream flow. The angle η is the acute angle between the local velocity vector and the local surface unit normal vector. This angle is determined from the expression

$$\cos \eta = \frac{\vec{V} \cdot \vec{n}}{|\vec{V}|}$$

so that, then,

$$C_p = 1.87 \left[\frac{\vec{V} \cdot \vec{n}}{|\vec{V}|} \right]^2 \qquad (17)$$

is used to calculate the surface pressure distribution. This value of C_p is substituted into the force equations and Newtonian force coefficients are computed. One precept of the theory is that the pressure is zero in the "shadowed" region; thus, in integrating the surface pressures, a limit is set at $\cos \eta = 0$, or $\eta = \frac{\pi}{2}$.

The dashed lines on Figures 5, 6, 7, and 8, pages 39 through 45, represent the results of the Newtonian computations. Inasmuch as all of the body planes chosen for comparison are on the conical part of the body, the Newtonian distributions are the same for all planes at a given angle of attack. This is occasioned by the fact that neither the velocity nor the unit normal vector are functions of the body length. While the functional relationship for the normal vector is different on the cone and on the spherical cap, the transition at the tangent point is continuous; hence, there are no radial changes in the pressure distribution other than indicated here.

The body positions for which the radial pressure distribution is presented are chosen primarily on the basis of the quantity of experimental data available at each position; and secondly, chosen to present an indication of the pressure variations with body length. The experimental data shown for a given plane are generally taken from one

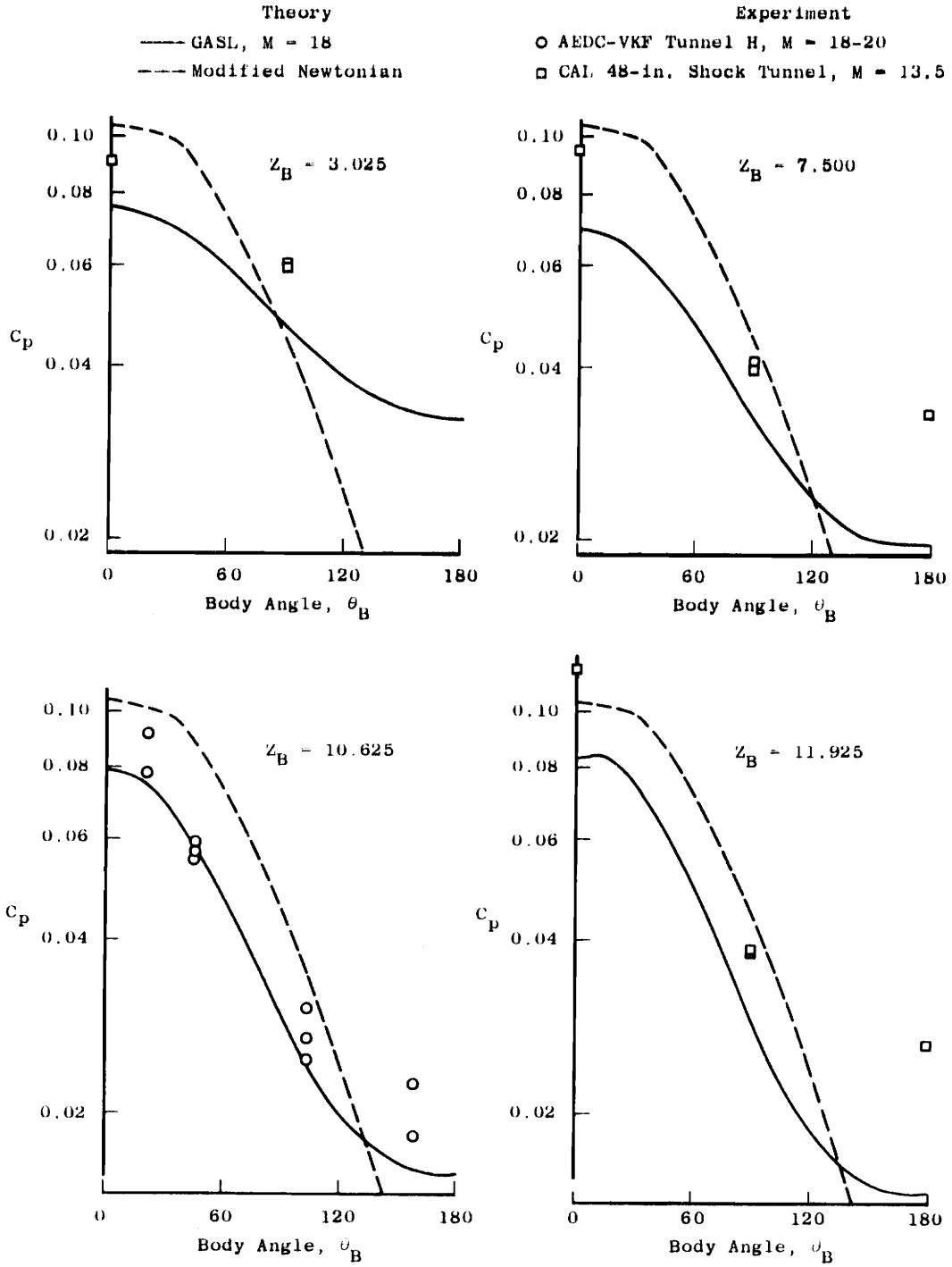

Figure 5. - Cone Radial Pressure Distributions for 5 Degrees Angle of Attack

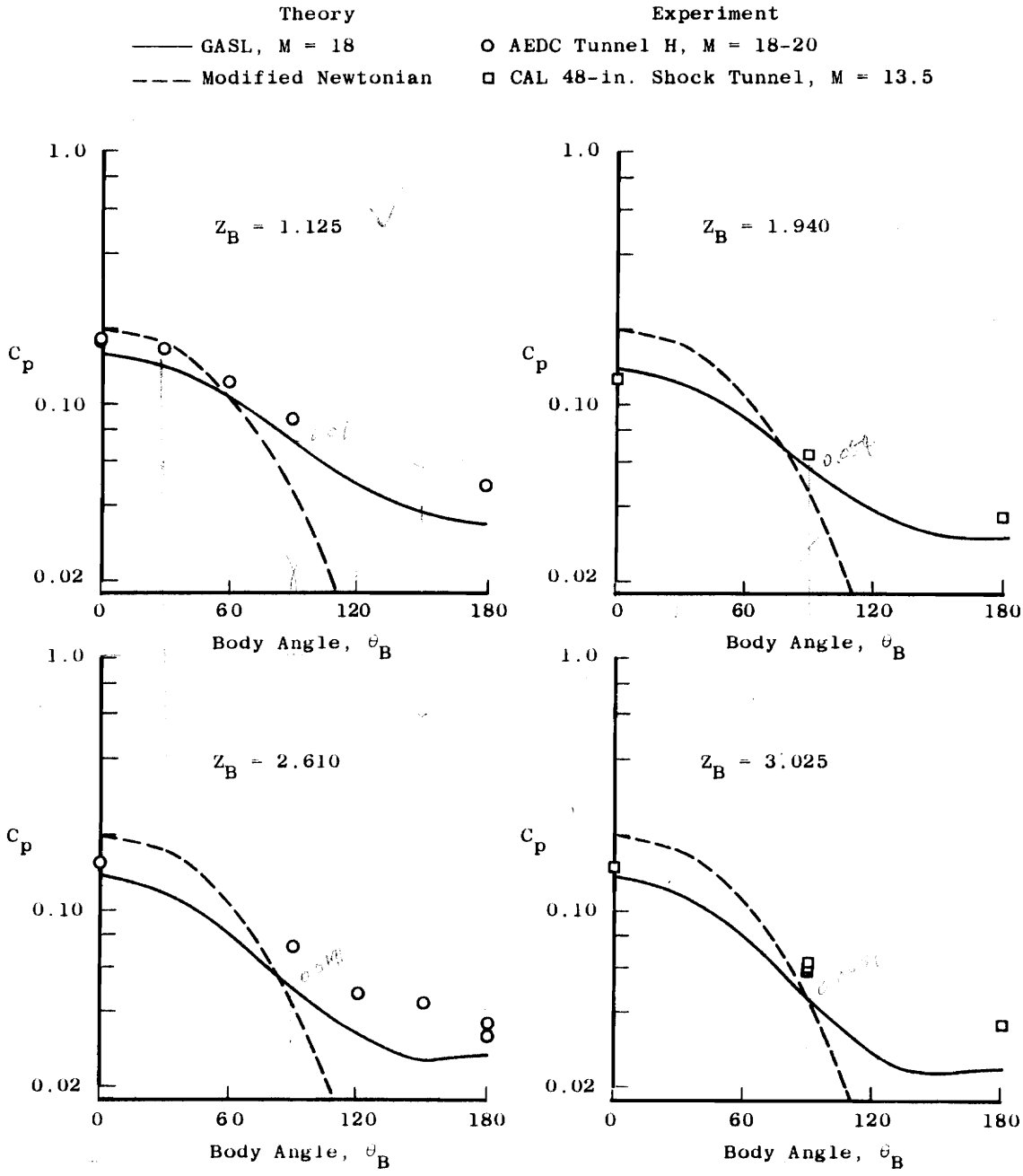

Figure 6. - Cone Radial Pressure Distributions for 10 Degrees Angle of Attack

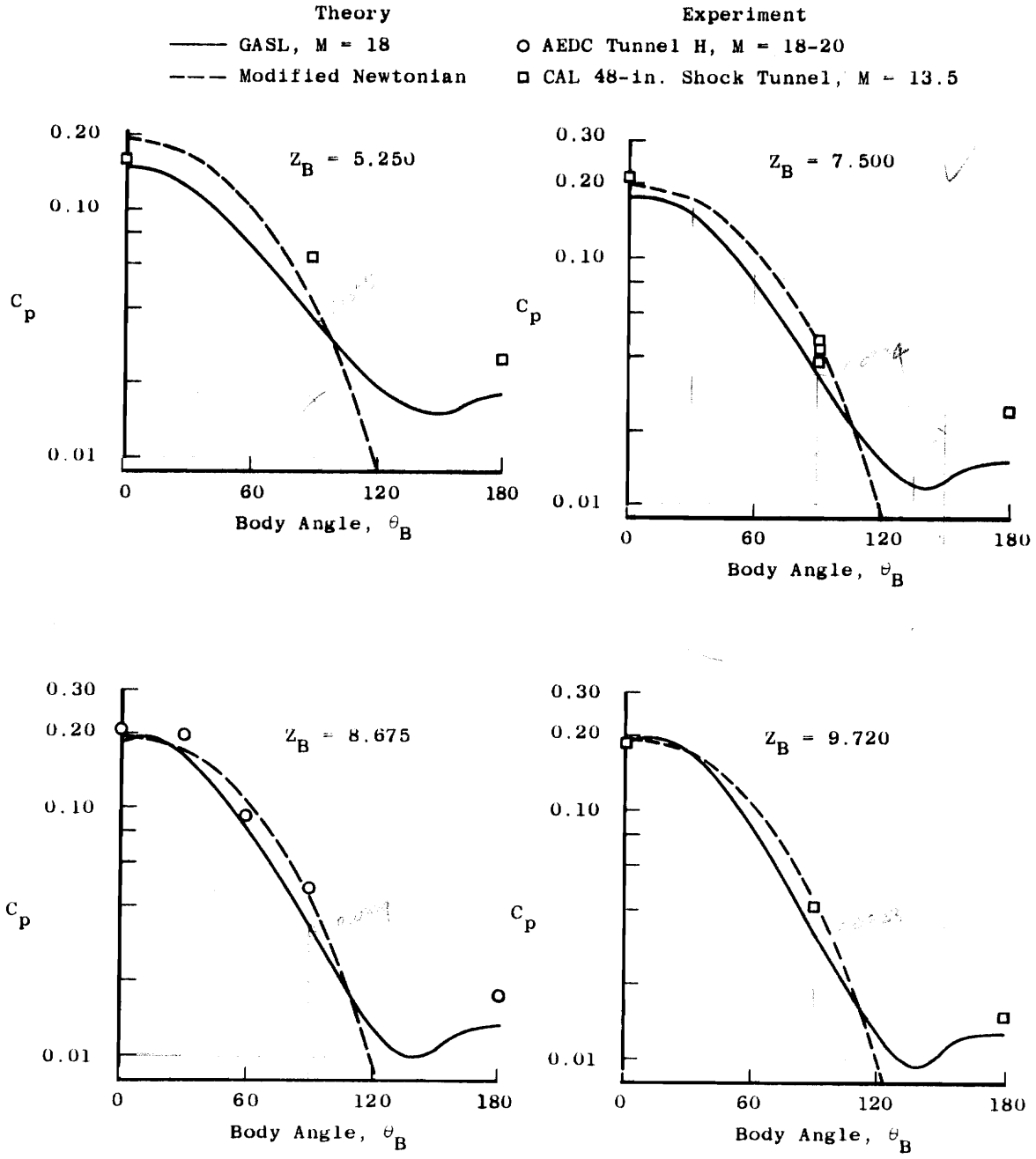

Figure 6.- Continued

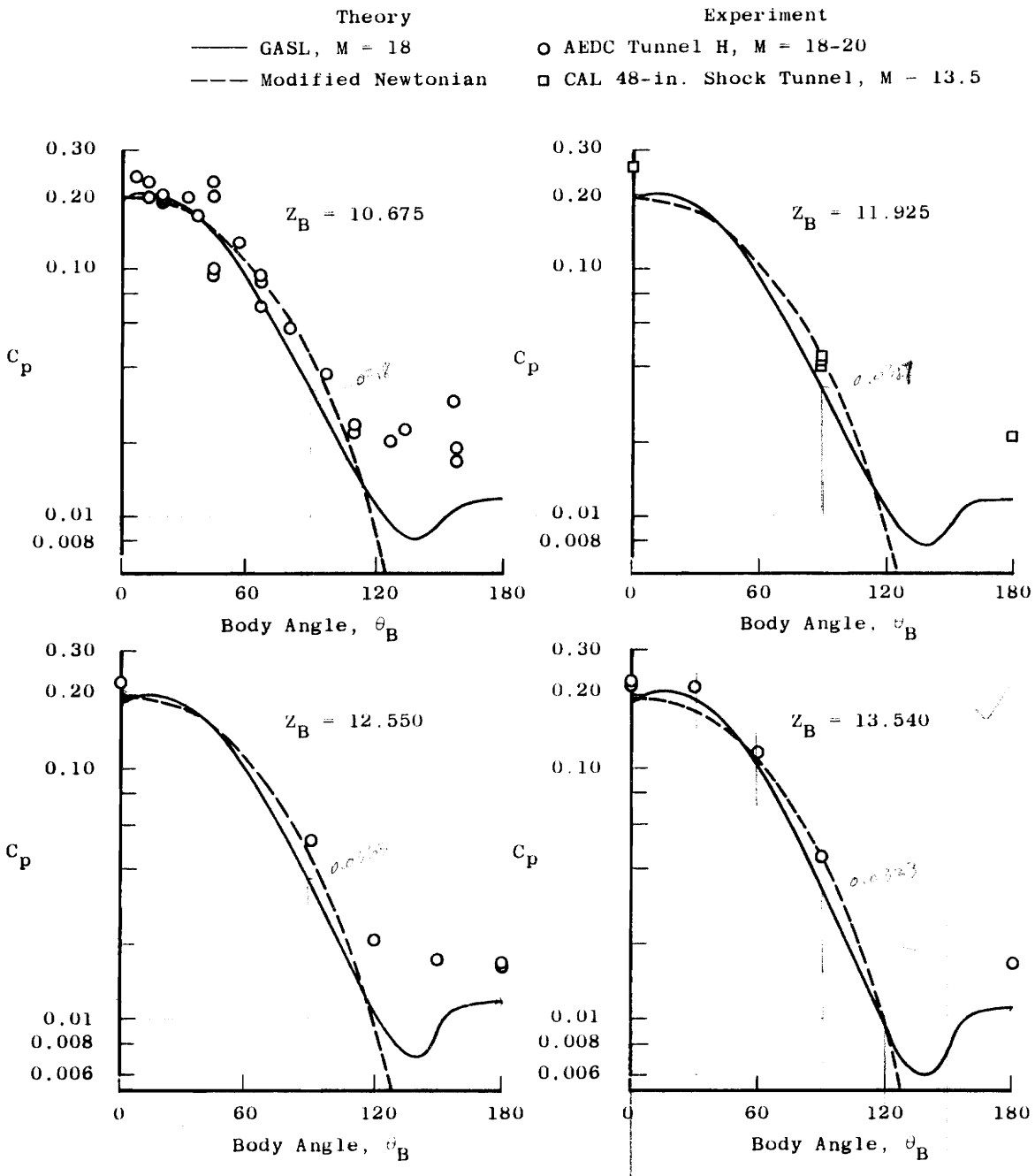

Figure 6. - Concluded

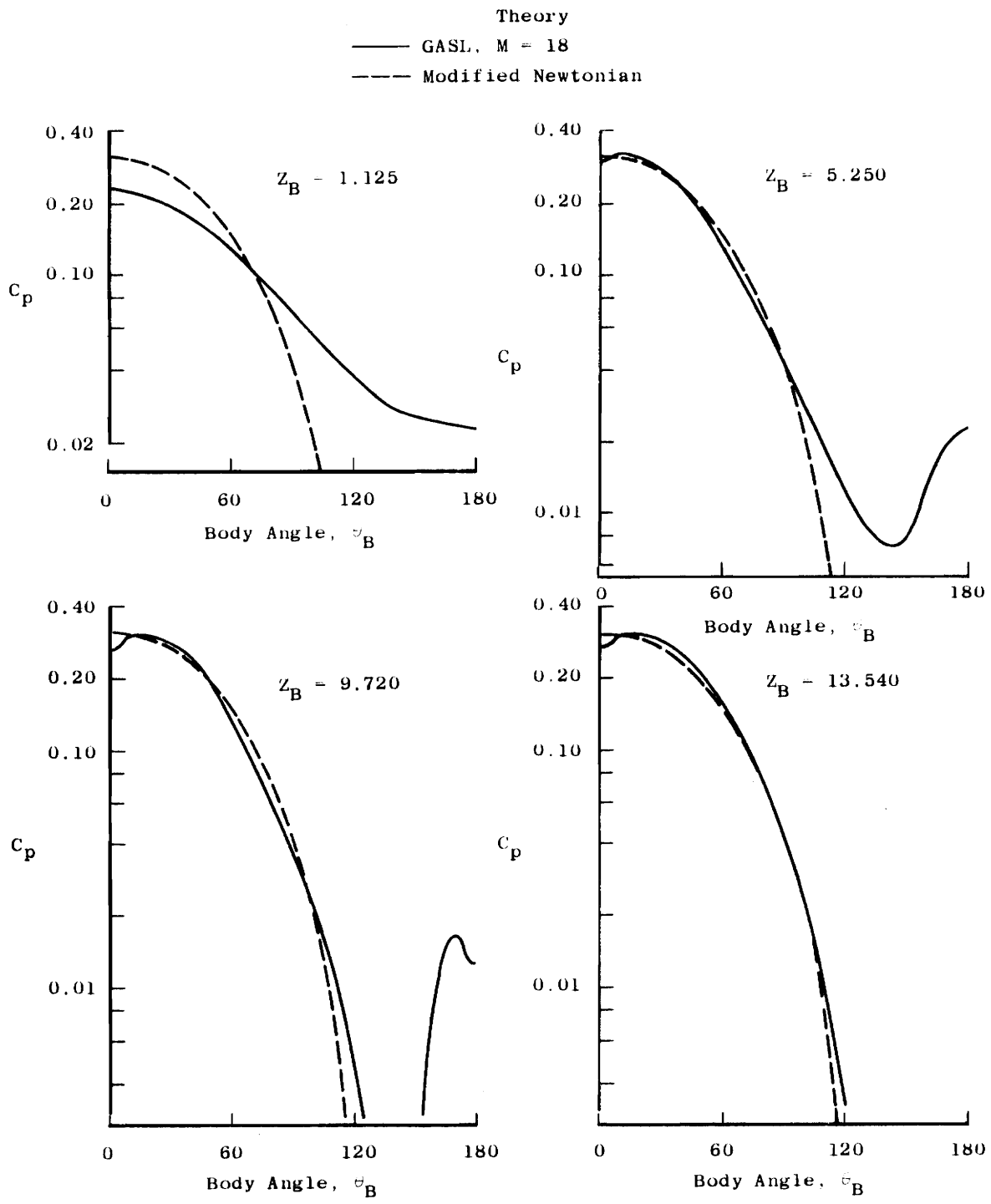

Figure 7. - Cone Radial Pressure Distributions for 15 Degrees Angle of Attack

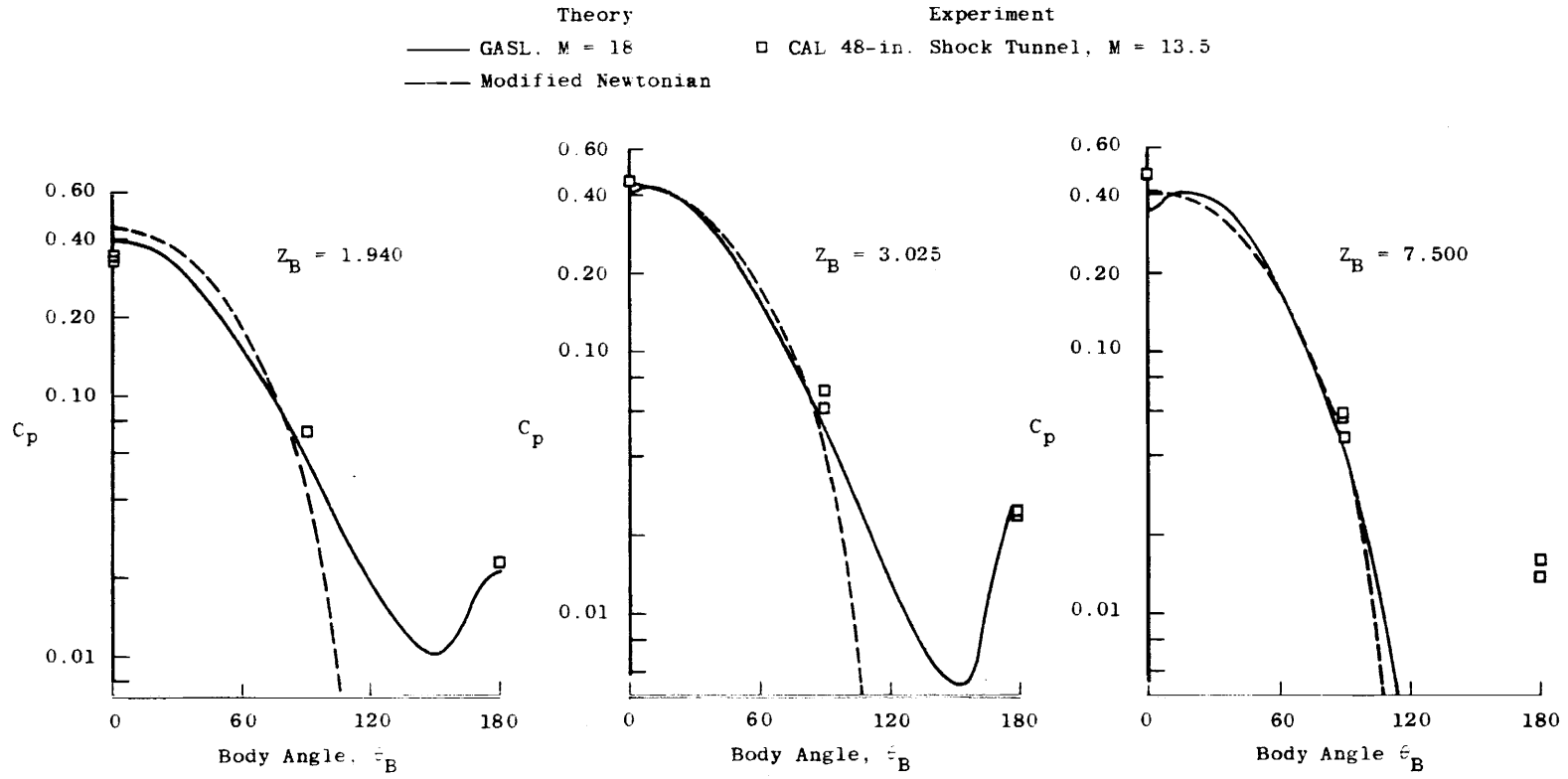

Figure 8. - Cone Radial Pressure Distributions for 20 Degrees Angle of Attack

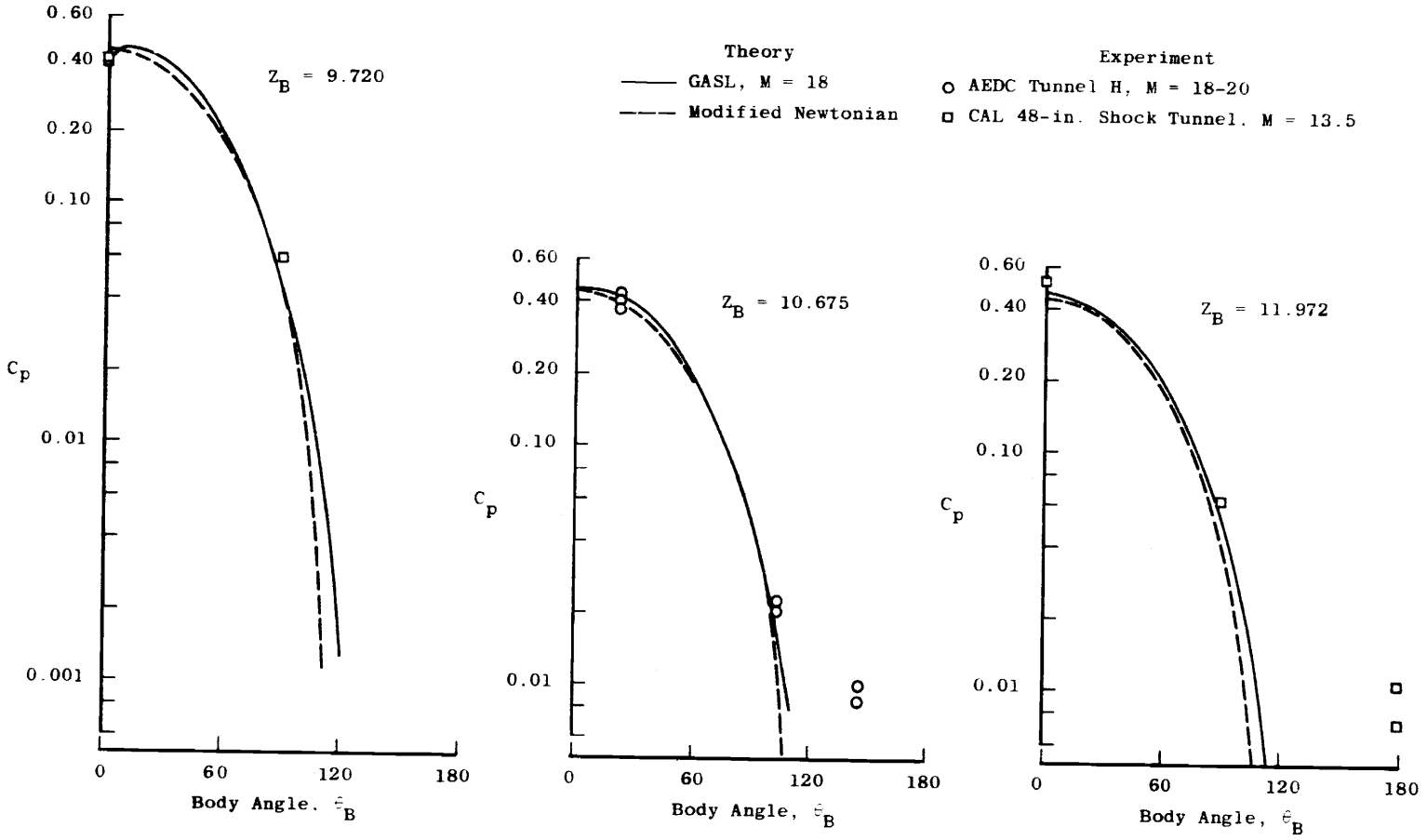

Figure 8. - Concluded

of the two sources, either AEDC-VKF or CAL. This precludes any mutual validation of the data by direct comparison. However, some indication of the agreement between the data is demonstrated in Figures 3 and 4, pages 30, 34, and 35, as well as by the report of Edenfield (15).

An examination of the distributions for all angles of attack suggests two primary results:

1. Notwithstanding the differences in some cases, the trends of the experimental and the GASL pressure distributions are very similar.
2. The modified Newtonian theory is totally inadequate for the task of predicting the pressure distribution on rather blunt slender bodies.

With regard to the first result, it is to be remembered that at low angles of attack the extraneous effects of viscous interaction strongly influence the experimental pressure distributions. Thus, for the 5-degree angle of attack case not much can be said except that the experimental and theoretical trends are similar, and that the experimental data are strongly affected by viscous effects.

The agreement is much improved for the 10-degree angle of attack case. Only on the leeward side is there any marked deviation between the GASL theory and experimental data. It is most difficult to determine the cause of this deviation since, on the one hand, the experimental results are subject to viscous effects, due to boundary-layer thickening in this region, while on the other hand, as the solution moves aft on the body a "well" of low pressure is developed

and followed by a large positive gradient to some higher pressure at the most leeward position. For increasing angles of attack, the "well" approaches a zero pressure and even becomes negative. The conditions of negative pressures are caused by the breakdown of the convergence criterion, and the solution fails shortly thereafter. It is necessary to exclude that region in any subsequent calculations further aft on the body. It is felt that both viscous effects and the effects of the "wells" are contributing to the indicated deviation; however, the validity of the idea of "wells" in the inviscid solution remains to be proven. One possible explanation for these "wells" is that as the flow on the windward side proceeds around the body, its velocity vector and/or streamlines move upward and away from the free-stream direction. However, as the leeward side of the body is approached, it is necessary for the flow from both sides to be turned back toward the free-stream direction, i.e., as the flow approaches the upper region of the vertical plane of symmetry, its sideward velocity component must approach zero. In order to do this, it appears that a high pressure ridge is required to retard the sideward motion and turn the flow. This explanation is plausible; however, a detailed examination by calculating streamline patterns for these pressure distributions and a comparison of mass conservation from one streamline to another is needed to show whether or not the pattern is realistic. Such an analysis is beyond the scope of this thesis; therefore, it will be said that this is a problem which needs further analysis.

It is also entirely plausible that the development of the

pressure "well" can be related to the relatively loose convergence criterion discussed earlier. The right-running characteristic on the leeward side is more nearly parallel to the body, particularly at higher angles of attack; thus the distance between intersections becomes larger, and the possibility of errors in the interpolations is increased. However, a detailed analysis of the program itself would be required to determine if any improvement could be obtained.

The 15-degree angle of attack case, presented in Figure 7, page 43, shows a further progression of the "wells" to the "cut off" point. At $Z_B = 5.25$ the "wells" have begun to form and at $Z_B = 9.72$ the bottom of the "well" has dropped to a value of practically zero (10^{-5}) with an almost infinitely positive gradient following. At stations further aft on the body the solution breaks down and finally fails. As a result, the leeward boundary condition is removed from the solution. The comparisons presented for the 20-degree angle of attack case show that the GASL program gives good results up to approximately the 90-degree station, without the leeward boundary condition, so it appears that no serious limitations on the solution are manifested on the windward side by the exclusion of regions on the leeward side of the body.

In the second result, what is meant by the statement of a "rather blunt slender body" is one with a comparatively small cone angle but with a large bluntness ratio; i.e., the overall body length is only a few nose radii. The previously observed trends in the pressure distributions are clearly observed near the nose of the body.

This region is subjected to overexpansion and subsequent recompressions which the modified Newtonian theory does not consider. Only for more slender bodies can the nose influence be diminished, and better agreement be obtained. The comparison presented here is considerably improved at the higher angles of attack, particularly on the windward side of the body, because the shock wave more closely approximates the shape of the body in this region. Therefore, because of the special circumstances which are necessary in order for modified Newtonian theory to apply, the use of this theory in predicting surface pressure distributions on general bodies is not considered reliable.

3. COMPARISON OF FORCE COEFFICIENTS

Having established that the GASL theory predicts the pressure distribution on a blunt slender cone at angle of attack, it remains to be shown whether or not the problems with the GASL solution in the leeward regions seriously impair the prediction of the inviscid force coefficients obtained by integrating the GASL pressure distributions with the "wells" included.

Since the experimental pressure data are known to be influenced by viscous action, it appears that some discussion of the effects and the magnitude of the viscous influence on the forces experienced by a body, and in particular a blunt slender cone, are warranted. This is necessary in order to make a more realistic evaluation of the comparisons between the theory and experimental data.

As was pointed out earlier, the work of Whitfield and Griffith (1) is related to this problem under conditions of zero yaw. It is felt that the effects revealed for zero yaw would be present at least qualitatively at angle of attack as well. Presented in Figure 9, page 51, is a reproduction of a figure from Reference (1) which shows the relative magnitudes of the various components which make up the total axial force on a cone at zero yaw. The axial force is presented as a function of a viscous parameter $\overline{\overline{v}}_\infty$, which is defined in Reference (1). A zero value of $\overline{\overline{v}}_\infty$ represents inviscid conditions and an increasing $\overline{\overline{v}}_\infty$ implies increased viscous effects. The range of $\overline{\overline{v}}_\infty$ for the data presented in this thesis is from 0.03 to 0.10. The significant aspect of this figure is that viscous effects can become a

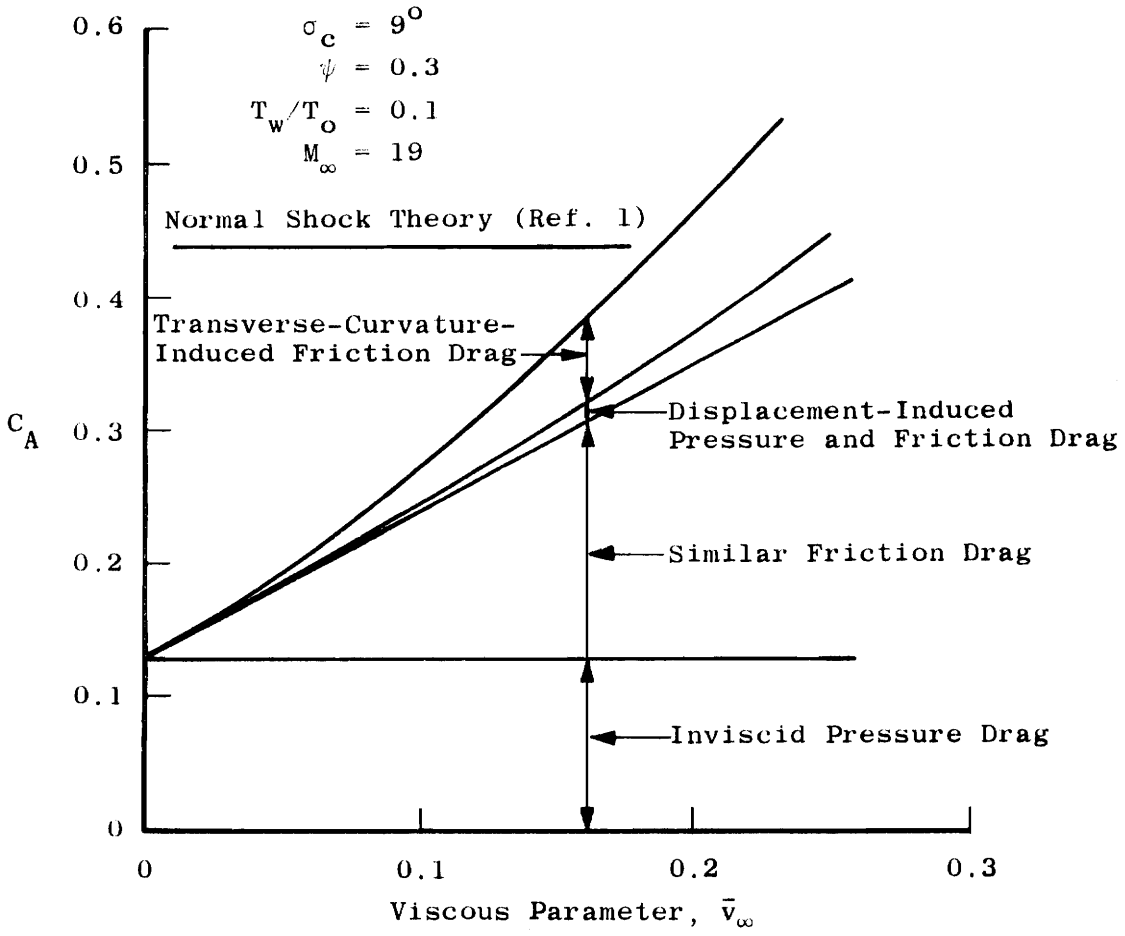

Figure 9. - Theoretical Drag Components for 9 Degree Blunt Cone

dominant factor in the drag experienced by a hypersonic vehicle, with boundary-layer friction drag being the largest of those effects. By comparison, the viscous-induced pressure distribution increment in the force is small.

Projecting these relative magnitudes to the angle of attack situation, the probable result is that the axial force is the most affected and the normal force is affected by a smaller amount. This can be attributed to the fact that the major viscous effect is due to the friction force.

The comparison of the computed and experimental force coefficients is presented in Figure 10, page 53. The experimental data were obtained for a viscous parameter value of 0.05. The comparisons presented for C_A indicate that viscous effects are most prevalent in the experimental data and that there appears to be a reasonable agreement between the Newtonian definition and the GASL results. Here again, even though there is a significant difference between experiment and theory, at least the trends are similar.

It is interesting to note that while reasonable agreement is obtained for C_A, the predictions obtained for the normal forces are markedly different, particularly at low angles of attack. These differences are amplified considerably in the L/D curve. Moreover, the experimental data for the normal force definitely tend toward the GASL results. The comparatively small increment that the experimental data rise above the GASL curve is attributed to the pressure-induced viscous effects. The deficiency indicated by the Newtonian results merely

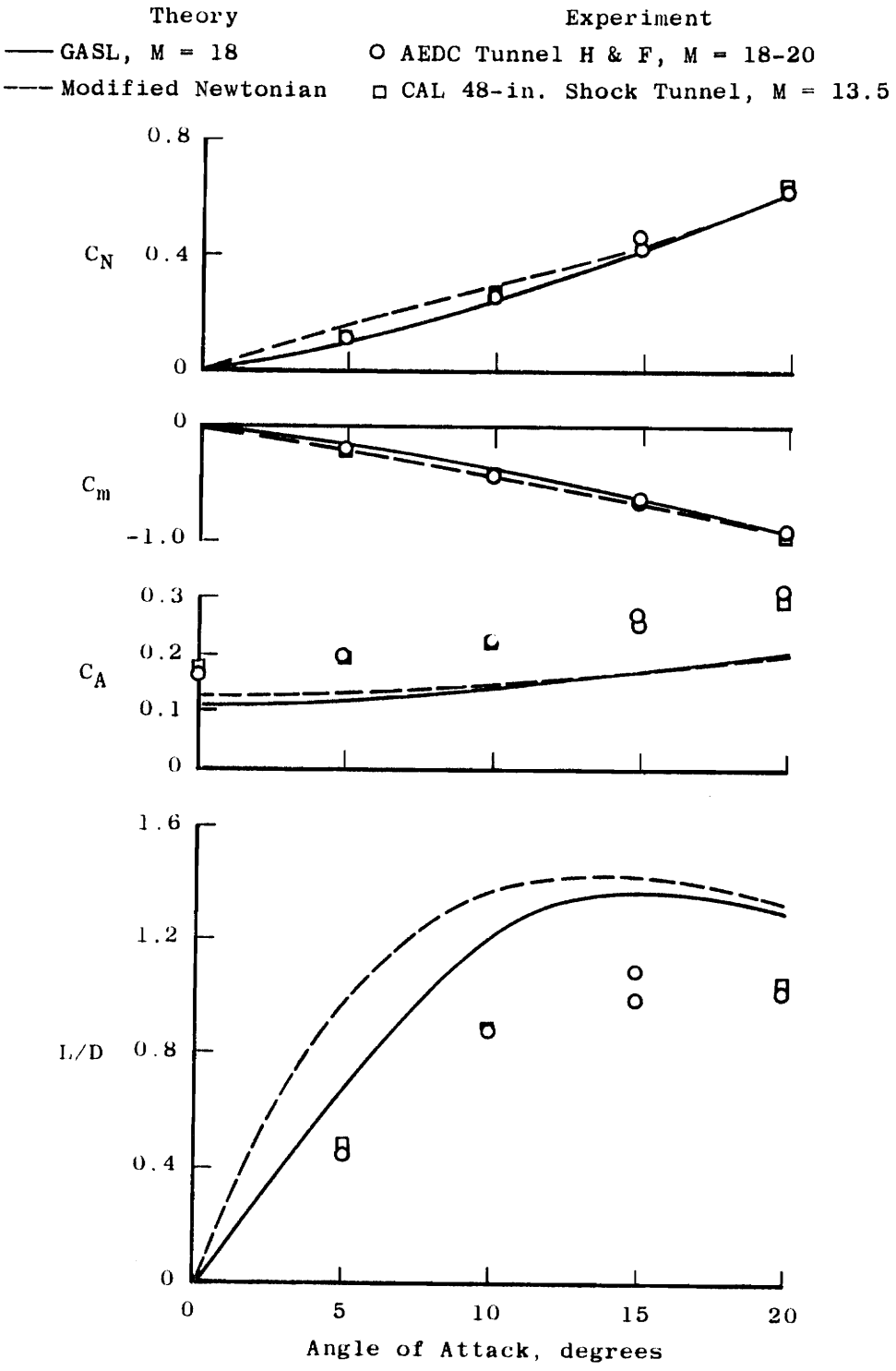

Figure 10. - Cone Force and Moment Coefficients

substantiates the results previously observed in comparing the pressure distributions.

Finally, the large differences between theory and experiment for the L/D curve are due mainly to the effect of the increased C_A values in the lift and drag equations. This effect decreases the lift while simultaneously increasing the drag value. These large differences indicate the penalty in performance that can be caused by viscous effects, and illustrates the necessity of understanding the underlying aspects of the viscous phenomena.

CHAPTER IV

CONCLUSIONS

Comparisons have been made between a general three-dimensional characteristics solution and available experimental data with regard to the pressure distributions and force and moment coefficients for a spherically-capped 9-degree semivertex angle circular cone, up to angles of attack of 20 degrees. Also, predictions were computed using modified Newtonian theory, since this theory has been widely used for bodies flying at hypersonic speeds. Several significant results have been found from these comparisons. These are briefly summarized in the following statements:

1. The GASL program is adequate to the task of predicting the inviscid pressure distribution and the resultant aerodynamic forces for bodies at angle of attack.
2. The irregularities that occur in the GASL solution on the leeward side of a body at large angle of attack may limit its applicability in its present form to small angles of attack. For the blunt cone body considered here it appears that a 10-degree angle of attack would be an upper limit of applicability.
3. The GASL program represents a new capability which can be employed to begin a more rigorous analysis of the viscous effects which are known to be prevalent in the hypersonic speed range.

4. Only under very special conditions is modified Newtonian theory useful. Inasmuch as these conditions are defined in only general terms, no reasonable range of applicability can be stated. In those cases where it is employed, reliability remains to be proven. In the present application the method was shown to be unreliable.

5. The GASL program represents a first step towards the ability to compute the supersonic inviscid flow field about bodies at angle of attack, both for the study of inviscid and viscous flow fields. However, if progress is to be made towards a complete understanding of these flow fields, the problems revealed in the present comparisons would indicate that much more research and analysis is required.

SUMMARY

Advances in computer technology have made it feasible to program on a high-speed computer the solution for the supersonic flow field about lifting bodies. The program developed by the General Applied Science Laboratories (GASL) represents an early solution in this field.

In this thesis, the GASL solution is compared with available experimental data and is found to be adequate for the task of predicting the inviscid pressure distribution on a lifting blunted cone. Moreover, the GASL program is considered to be a possible significant aid in the analysis of viscous interaction effects at hypersonic speeds. Similarly, comparisons are made with modified Newtonian theory which indicate that this theory is not reliable, except under special conditions.

BIBLIOGRAPHY

BIBLIOGRAPHY

1. J. D. Whitfield and B. J. Griffith, "Viscous Effects on Zero-Lift Drag of Slender Blunt Cones," Arnold Engineering Development Center TDR-63-35, March, 1963.

2. G. Moretti, E. A. Sanlorenzo, E. E. Magnus, and G. Weilerstein, "Supersonic Flow About General Three-Dimensional Bodies," Vol. III: Flow Field Analysis of Reentry Configurations by a General Three-Dimensional Method of Characteristics," TDR-61-727, Aeronautical Systems Division, USAF, October, 1962.

3. L. R. Fowell, "Flow Field Analysis for Lifting Re-Entry Configurations by the Method of Characteristics," IAS Paper No. 61-208-1902, Joint IAS-ARS Meeting, June, 1961.

4. A. Ferri and Vaglio - Laurin, "External Hypersonic Flows," Aerospace Engineering, Vol. 22, No. 1, January, 1963.

5. Space-General Corporation, Private Communications.

6. M. van Dyke, "The Supersonic Blunt Body Problem - Review and Extensions," Journal of Aerospace Sciences, Vol. 25, pp. 485-496, 1958.

7. J. Lukasiewicz, R. Jackson, and J. Whitfield, "Status of Development of Hotshot Tunnels at the AEDC." Paper presented at the AGARD Meeting on "High Temperature Aspects of Hypersonic Flow," Training Center for Experimental Aerodynamics, Rhode-Saint-Genese, Belgium, April 3-6, 1962. van der Bliek, J. A. "Further Development of Capacitance and Inductance Driven Hotshot Tunnels," Arnold Engineering Development Center TDR-62-50, March, 1962.

8. W. E. Smotherman, "A Miniature Wafer-Style Pressure Transducer," Arnold Engineering Development Center TR-60-11, October, 1960.

9. E. E. Edenfield and R. L. Ledford, "Compensation of Dynamic Sting Effects in Hotshot Force Measurements," Arnold Engineering Development Center TDR-62-122, June, 1962.

10. W. T. Earheart and D. S. Bynum, "Hypervelocity Arc-Tunnel Instrumentation," Arnold Engineering Development Center TN-60-227, December, 1960.

11. M. Grabau, R. L. Humphrey, and W. J. Little, "Determination of Test Section, After-Shock, and Stagnation Conditions in Hotshot Tunnels Using Real Nitrogen at Temperatures from 3000 to 4000°K," Arnold Engineering Development Center TN-61-82, July, 1961.

12. "CAL 48-inch Hypersonic Shock Tunnel Description and Capabilities," Cornell Aeronautical Laboratory, Buffalo, New York, May, 1962.

13. J. F. Martin, G. R. Duryea, and L. M. Stevenson, "Instrumentation for Force and Pressure Measurements in a Hypersonic Shock Tunnel," Cornell Aeronautical Laboratory Report No. 113, January, 1962.

14. D. B. Wilkinson and S. A. Harrington, "Hypersonic Force, Pressure and Heat Transfer Investigations of Sharp and Blunt Slender Cones," Arnold Engineering Development Center TDR-63-177, August, 1963.

15. E. E. Edenfield, "Comparison of Hotshot Tunnel Force, Pressure, Heat Transfer and Shock Shape Data with Shock Tunnel Data," Arnold Engineering Development Center TDR-64-1, January, 1964.

16. B. J. Griffith and C. H. Lewis, "Laminar Heat Transfer to Spherically Blunted Cones at Hypersonic Conditions," Journal of American Institute of Aeronautics and Astronautics, Vol. 2, No. 3, March, 1964.

17. R. F. Probstein, "Interacting Hypersonic Laminar Boundary Layer Flow Over a Cone," Tech. Report AF2798/1, Division of Engineering, Brown University, AD66 227, March, 1955.

VITA

The candidate was born in Atlanta, Georgia, November 22, 1934; received his grade schooling in the public schools there, and secondary education at Saint Andrew's School, St. Andrews, Tennessee, a boys boarding school administered by an order of Episcopalian monks, the Order of the Holy Cross, West Park, New York.

The candidate spent 2-1/2 years at Emory University as a mathematics major before attending the Georgia Institute of Technology for 2-1/2 years and graduating with a Bachelor of Science Degree in Aeronautical Engineering in June, 1957.

The next 4-1/2 years were spent in employment at the Langley Research Center of the National Aeronautics and Space Administration, during which time the course work of this program was completed. The candidate next took employment and is presently working at Arnold Engineering Development Center for ARO, Inc. At the beginning of the year, 1964, support was given by ARO, Inc. for the work which is described in this thesis.

A CRITICAL COMPARISON OF COMPUTED AND EXPERIMENTAL PRESSURE DISTRIBUTIONS AND FORCE COEFFICIENTS ON A BLUNTED-CONE AT ANGLE OF ATTACK

By Eugene C. Knox, Thesis submitted in candidacy for the degree of MASTER OF SCIENCE in Aerospace Engineering, Virginia Polytechnic Institute, Blacksburg, Virginia, December 1964.

ABSTRACT

Advances in computer technology have made it feasible to program on a high-speed computer the solution for the supersonic flow field about lifting bodies. The program developed by the General Applied Science Laboratories (GASL) represents an early solution in this field.

In this thesis, the GASL solution is compared with some available experimental data and is found to be adequate for the task of predicting the inviscid pressure distribution on a lifting blunted cone. Moreover, the GASL program is considered to be a potentially significant aid in the analysis of viscous interaction effects at hypersonic speeds. Similarly, comparisons are made with modified Newtonian theory which indicate that this theory is not reliable, except under special conditions.